Active Physicalization of Temporal Bone

Fatemeh Yazdanbakhsh[a] and Faramarz Samavati[b]
Department of Computer Science, University of Calgary, Calgary, Alberta, Canada

Keywords: Physicalization, Active Physicalization, Interactive, Touch Sensor, 3D Printing.

Abstract: This paper explores the integration of conductivity, electricity, controllers, and 3D printing technologies to develop an active physicalization model. The model is interactive and utilizes conductive 3D filaments as sensors to trigger a feedback system when activated. The resulting interactive model can be applied to various physicalized models where the internal structure is crucial. As a case study, we have 3D printed a temporal bone model with its inner organs, using conductive material to sense the proximity of a drill around the inner organs. When a surgical drill comes into contact with these conductive-material-printed inner organs, it triggers the feedback system, producing feedback in the form of a buzzer or blinking LED. Our adaptable feedback system extends beyond surgery rehearsal, with the case study serving as a representative example.

1 INTRODUCTION

Physicalization is defined as a "physical artifact, the geometry or material properties of which encode data" or in other words, physical representation of data (Jansen et al., 2015). Physicalization offers significant benefits by transforming abstract data into tangible forms, enhancing understanding of data and engagement of working with data. One major advantage is the ability to interact physically with data, allowing users to touch, manipulate, and explore information in ways that digital screens cannot provide. This tactile interaction stimulates multiple senses, enhancing both the understanding and retention of complex information. Additionally, physical models serve as intuitive tools for communicating intricate data to non-experts, making abstract concepts more accessible. Moreover, physicalization promotes collaborative exploration and discussion, as physical artifacts can be easily shared and examined in group settings. This collaborative aspect enhances the communication of ideas and supports team-based problem-solving (Huron et al., 2017).

Physicalization is divided into three categories: passive, augmented and active (Djavaherpour et al., 2021). Passive physicalization is defined as using digital fabrication devices to create a static object without any enhanced interaction; in contrast, augmented physicalization is defined as a combination of data physicalization usually passive and augmented reality (AR) techniques. Active physicalization usually involves other sources of energy like electricity to create more interactive movements and actions. These are usually controlled with a microcontroller.

Unlike passive physicalizations, active physicalizations offer several distinct advantages. They enable the visualization of evolving datasets (Pahr et al., 2024), allowing users to observe changes and trends over time (Barbosa et al., 2023; Sauvé et al., 2020). This capability is particularly beneficial in applications where real-time monitoring is crucial, such as in biological and medical diagnostics (Roo et al., 2020; Karolus et al., 2021), environmental monitoring (Houben et al., 2016), and interactive art installations (LOZANO-HEMMER, 2011). Active physicalizations can also support enhanced interactivity, enabling users to manipulate data through physical interfaces, thus fostering a more engaging data exploration experience.

Overall, active physicalization bridges the gap between the digital and physical worlds, offering a powerful medium for data interaction and interpretation.

In 3D printing as a common method for fabricating passive physicalization, it is sometimes crucial to accurately replicating inner structures, specially when reproducing medical organs with intricate inner structures and vessels (Bao et al., 2023; Sun et al., 2023; Tan et al., 2022). For example for medical surgery rehearsal and education purposes, there have been many interests in using physicalization for temporal bone

[a] https://orcid.org/0000-0002-1082-6522
[b] https://orcid.org/0000-0001-9440-7562

Yazdanbakhsh, F. and Samavati, F.
Active Physicalization of Temporal Bone.
DOI: 10.5220/0013160200003912

In *Proceedings of the 20th International Joint Conference on Computer Vision, Imaging and Computer Graphics Theory and Applications (VISIGRAPP 2025) - Volume 1: GRAPP, HUCAPP and IVAPP*, pages 903-912
ISBN: 978-989-758-728-3; ISSN: 2184-4321

(Ang et al., 2024; Iannella et al., 2024; Freiser et al., 2019; Rose et al., 2015; Suzuki et al., 2018; Cohen and Reyes, 2015), brain (Jeising et al., 2024; Huang et al., 2019; Guo et al., 2020) and dental (Domysche et al., 2024; Reich et al., 2022; Park et al., 2019; Hou et al., 2024) surgery. The internal structure in these works is commonly revealed or displayed through drilling or cutting, as exemplified in (Longfield et al., 2015; Cohen and Reyes, 2015), where organs are dissected to show the inner structure and measure them. Another method to display inner organs involves using transparent external structures, such as in the work by (Suzuki et al., 2018), where the temporal bone is made transparent, allowing the inner organs to be seen in color and their proportions to be visible. Additionally, some approaches print the organ as several disassembled parts, making it easy to measure and observe the inner organs in the cut areas, as utilized in (Wanibuchi et al., 2016) for surgical training.

When employing cutting methods for surgical simulations and educational purposes, the precision of the internal structures and their spatial relationships with the external structures become critical. Moreover, it is crucial to have a means to guide the cutting process when in contact with the internal structures, necessitating supportive actions and the implementation of active physicalization.

In this work, we introduce an active physicalization of the temporal bone to facilitate interaction with the critical internal organs. Based on the welling-scale criteria outlined in (Wan et al., 2010), certain inner organs (i.e. sigmoid sinus, facial nerve, inner ear) should remain untouched during surgery. In our active physicalization, during the cutting or drilling of internal structures, or when the drill is in proximity of these structures, a *warning action* such as a buzzer sound or an LED light, is triggered. We use affordable 3D printers, Raspberry Pi, and off-the-shelf conductive 3D printing material for our physicalizations. The sensors are designed using conductive materials and connected to the internal structures. We utilized a simple circuit controlled by Raspberry Pi to activate the warning actions when the drill tip touches the internal structures.

The complexity of using ready-to-use sensors encouraged us to design a self-designed sensor. Using ready-to-use sensors in small structures presents significant challenges due to their standardized sizes, shapes, and power needs. Furthermore, integration complexity and insufficient sensitivity add to the difficulties. Our custom-designed sensors offer precise tailoring to the specific size, shape and performance requirements of the application.

To create the 3D printed model of temporal bone, we need to address several challenges. For instance, selecting the materials that can better simulate bone and inner organs; 3D printing using multi-color and multi-material; recreating small and complex inner organs precisely; removing extra material from the hollow spaces present in temporal bone datasets. The type of printer plays an important role in choosing the appropriate material. We print the main bone parts with white PETG (won't be melt when drilled away) and the inner organs with special PLA to sense the proximity of drill to the inner organs using affordable 3D printers.

An additional challenge with this design is to ensure that the circuit initiates the warning action when the drill tip is close to the internal structure, just before touching or cutting the critical internal organ. To address this challenge, we strategically offset the selected internal organs. We then implemented our sensor circuit, attaching it to this offset region. This approach allows for precise monitoring and warning the user before the actual inner structure is touched.

The main contribution of this work includes:

- Active physicalization of temporal bone
- Warning system integration
- Custom sensor design for active physicalization of objects with complex internal structures

Section 2 delves into some of the related works. Section 2.2, covers different types of physcalization and example of them. In Section 4, you will find detailed information about the conductive PLA used in the experiment and the circuit design in Section 4. The conclusion can be found in Section 6.

2 BACKGROUND AND RELATED WORK

In this section, we review some of the state of the arts papers in regard to physicalization and physicalization of temporal bone.

2.1 Temporal Bone Anatomy

The temporal bone is a highly complex structure within the skull that houses several critical anatomical features, making it a focal point in surgical procedures like mastoidectomy, which is often performed to treat chronic infections. During this procedure, the temporal bone is dissected, and sometimes a cochlear implant is placed to restore hearing. This bone contains essential structures, including the facial nerve and the sigmoid sinus, among others, which must be preserved to avoid severe complications.

The facial nerve is responsible for controlling the muscles of facial expression, and damage to this nerve can result in facial paralysis. The sigmoid sinus, a major venous channel, is crucial for draining blood from the brain; any injury to it can lead to significant bleeding and potentially fatal outcomes. Ensuring the safety and integrity of these structures during mastoidectomy is paramount to maintain the patient's health and functionality. To aid in understanding the complex anatomy of the temporal bone, a comprehensive atlas of images detailing its structure is provided (Lane and Witte, 2009). Additionally, the Otolaryngology Department of Stanford University offers a graphical atlas of ear and temporal bone anatomy, available at (Jackler and Gralapp, 2024), which serves as educational tool for both students and professionals. Moreover, embracing other visualization tools can enhance the understanding of the temporal bone's intricate structures. Moreover, embracing other visualization tools can enhance the understanding of the temporal bone's intricate structure.

2.2 Physicalization

Physicalization, encompassing passive, augmented, and active forms, has become increasingly important in the medical field for enhancing the understanding and interaction with complex data. Passive physicalization involves creating tangible models from data, such as using 4D flow MRI images to represent blood flow (Ang et al., 2019) or 3D printing resin-based artificial teeth for dentistry (Chung et al., 2018). To address the challenge of large models exceeding 3D printer capacities, methods like segmenting large geospatial models into smaller parts have been developed (Allahverdi et al., 2018), and multiscale representations of historical sites have been created (Etemad et al., 2023).

Augmented physicalization, or mixed reality, combines physical models with virtual information to enhance utility. For example, the integration of AR with 3D-printed anatomical models (McJunkin et al., 2018; Barber et al., 2018; Mossman et al., 2023) uses platforms such as Unity (Haas, 2014) and ITK-SNAP for organ segmentation (Yushkevich et al., 2006). Active physicalization, a form of interaction design where physical objects change shape in response to data or environmental stimuli, has been explored in various fields. In art installations, for instance, actuated tape measures (LOZANO-HEMMER, 2011) is used to create immersive, responsive environments by dynamically reacting to the presence and movement of people. These installations exemplify how physical objects can actively respond to their surroundings. Similarly, platforms developed for active physicalization often incorporate features from web-based visualization tools, such as search, filtering, and highlighting, offering a comprehensive and versatile approach to data representation (Djavaherpour et al., 2021). In the biomedical field, shape-changing interfaces, such as the one introduced in (Boem and Iwata, 2018), enable remote monitoring of vital signs, allowing individuals to perceive real-time health data of a hospitalized person through tactile shape changes.

These applications of physicalization and mixed reality within the medical domain offer detailed representations and interactive enhancements, proving invaluable for education, diagnosis, and treatment planning. The following section explores state-of-the-art methodologies and innovations in this rapidly evolving area.

2.3 Temporal Bone Physicalization

The physicalization of the temporal bone holds significant potential in surgery training and planning, drawing the attention of numerous researchers.

Several studies utilize FDM 3D printers Haffner et al. (Haffner et al., 2018) experimented with various materials, including PLA, ABS, nylon, PETG, and PC, finding that PETG provided the best haptic feedback and appearance. Cohen et al. (Cohen and Reyes, 2015) printed models using ABS filament, noting that while the qualitative feel of ABS was softer than bone, the resulting dust was similar to bone.

Resin-based printers have also been utilized. Suzuki et al. (Suzuki et al., 2018) created a scale model using transparent and white resin to reconstruct the temporal bone and vestibulocochlear organ. Freiser et al. (Freiser et al., 2019) used white acrylic resin, finding moderate similarity in tactile sense to human bone. Additionally, Rose et al. (Rose et al., 2015) employed multi-material printing with varying polymer ratios for surgery planning, measuring accuracy in terms of absolute and relative distances.

SLS 3D printers are another approach. Longfield et al. (Longfield et al., 2015) developed affordable pediatric temporal bone models using multiple-color printing. Takahashi et al. (Takahashi et al., 2017) used plaster powder to reproduce most structures, except for the stapes, tympanic sinus, and mastoid air cells. Hochman et al. (Hochman et al., 2014) tested different infiltrants to achieve high internal anatomic fidelity in their rapid-prototyped models.

In comparison, our active physicalization model offers several advantages. Unlike the passive models that focus on static representations, our model integrates interactive elements, providing dynamic feedback and enhancing the surgical planning and training experience. This approach not only improves the anatomical accuracy and tactile feel but also allows for the simulation of various surgical scenarios, thereby may offer a more comprehensive training tool for medical professionals.

3 TEMPORAL BONE 3D MODEL

The temporal bone model in this work was created using micro CT scan data with a resolution of $0.154mm$ and $570 \times 506 \times 583$ dimensions. The datasets are private and come from researchers at the University of Calgary and Western University. The micro CT scans were converted into a 3D model via the Visualization toolkit (Schroeder et al., 2004). The model was segmented using 3D-slicer's semi-automatic feature segmentation (Fedorov et al., 2012), isolating the main bone by adjusting the intensity thresholds based on the Hounsfield unit (ScienceDirect, 2024). Post segmentation review led to further manual segmentation to reduce artifacts and include missing areas. The final segmentation was converted to STL format for 3D printing. Figure 1.(a-c) shows the axial, coronal, and sagittal views of the temporal bone along with the segmentation of inner organs. Figure 1.(d-e) demonstrates the final segmentation of the temporal bone and its 3D-printed version. We opted to use the

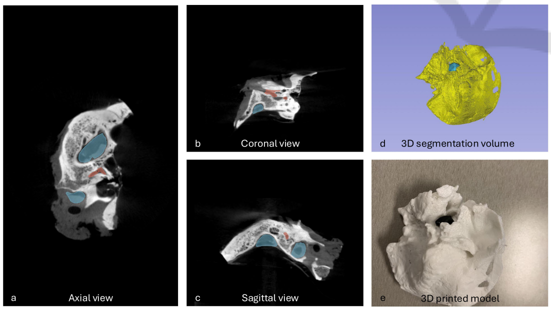

Figure 1: Axial, coronal, and sagittal views of the temporal bone with organ segmentation (a-c), and final segmentation with 3D-printed model (d-e).

MakerGear M3-ID, a dual extruder Fused Deposition Modeling (FDM) printer chosen for its affordability and practicality in our research. This choice ensures that our methods are reproducible and accessible to others in the field. The printer's bed size adequately accommodates our fabrication needs for the size of objects we intend to create. The 3D-printed model is shown in Figure 2, with the partially printed bone on the left, fully printed on the right, and its mapping to the human head in the center. White PETG was used for the main bone structure due to its reported similarity to bone texture when printed (Haffner et al., 2018), while black conductive PLA was selected for the inner organs for its conductivity and clean finish, making it suitable for our feedback system and easier to print compared to materials like ABS.

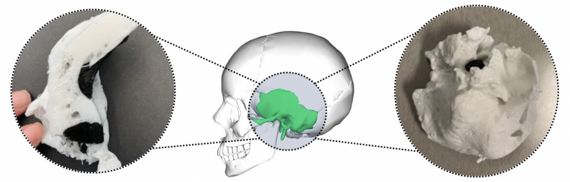

Figure 2: 3D-printed model: partially printed (left), fully printed (right), and mapped to the human head (center). White PETG is used for printing bone, black conductive PLA for inner organs including facial nerve, and sigmoid sinus.

4 DESIGN AND IMPLEMENTATION OF WARNING SYSTEM

In cochlear implant surgery, it is crucial to avoid contact with certain internal organs due to the severe and irreversible risks associated with their disturbance. Critical inner organs, such as the sigmoid sinus and the facial nerve, must be handled with extreme care. These organs present a unique challenge due to their complex structures and their locations, often hidden or covered by bones. To aid in navigating these complexities, we have designed and implemented a warning system in our active physicalization specifically for these two organs.

The main application of this feedback system is to evaluate the intactness of inner organs, including the sigmoid sinus and the facial nerve. The feedback system utilizes embedded sensors in the 3D-printed model. These sensors provide feedback, such as buzzer sounds or flashing lights, to notify the users when they are cutting part of the anatomy that should not be disturbed.

Instead of using off-the-shelf sensors, which can be challenging to integrate into rigid 3D-printed objects, we opted for self-designed sensors. These custom sensors offer the flexibility to adjust their size according to specific requirements, incorporating parts of the 3D-printed object itself into the sensor design.

We designed a circuit to activate an LED/buzzer. The circuit consists of hardware components such as resistors, batteries, and wires. However, instead of traditional metal wires covered with plastic insulation, we used conductive PLA to function as the wires. PLA-made wires are more convenient to embed within a 3D-printed model due to their flexibility in shape and size. Therefore, we employed conductive PLA to design the connections that allow current to flow through the circuit. Current-conductive PLA material is suitable for printing these connectors (Kwok et al., 2017; Flowers et al., 2017). In this work, we utilized Carbon Fiber Reinforced PLA (Proto-Pasta) for printing the segmentation of the inner organs.

The standard measurement used to characterize a conductive material is volume resistivity, measured in ohm-cm units. It is the resistance through a one-centimeter cube of conductive material. The resistance of the Proto-Pasta material is reported as follows:

- Volume resistivity of 3D-printed parts perpendicular to layers: 30 ohm-cm
- Volume resistivity of 3D-printed parts through layers (along the Z-axis): 115 ohm-cm

This volume resistivity data guides us in selecting appropriate resistors for our circuits, a topic further elaborated in section 4.1, which details the circuit design process.

4.1 Designing the Circuit

In this subsection, we outline the design of the proposed self-designed sensor utilizing conductive PLA. As discussed, in the first step, we create a 3D-printed temporal bone using two distinct materials. The non-conductive material (PETG) is employed to fabricate the temporal bone structure, while the conductive material (PLA) is utilized for the inner organs. Protecting these inner organs against drilling is significantly important; therefore, the feedback system needs to be designed with this consideration in mind. Printing the inner organs with conductive material enables us to use them as part of an electrical circuit, thereby creating feedback. Figure 3 illustrates how the conductive elements function as wires in our circuit, facilitating the flow of electrical current upon circuit closure.

To develop a flexible and general warning feedback system, we utilized a Raspberry Pi and a modified drill in the circuit. The modified drill has been designed and connected to the circuit to serve as a sensing tool for the internal material, providing real-time feedback on material changes during the drilling. This setup allows for various warning systems, such as activating a sound player for verbal instructions, activating a buzzer, or blinking LEDs. The circuit is designed as an open circuit, which closes when the drill touches the conductive inner organs. Upon contact, the circuit closes, and electricity flows through the system, triggering the buzzer by sending high voltage to the GPIO pin responsible for triggering the feedback system. A GPIO gate on a Raspberry Pi refers to the functionality of its GPIO pins. These pins facilitate the board's interaction with external hardware, allowing for programmability to either read signals from a sensor (input) or control devices such as LEDs and buzzers (output).

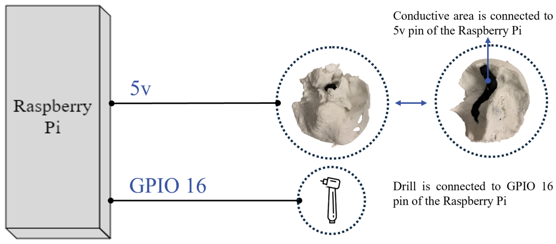

Figure 3: Simplified design of the sensor.

4.2 Offsetting Internal Organs

One of the challenges is ensuring that the circuit provides a warning when the drill tip is near critical organs. We address this challenge by offsetting the organs and connecting the sensor circuit to this offset region. To achieve this, we use a conductive material for the offset region. First, we read the main bone mesh and the inner organs mesh, followed by performing a 3D dilation of the inner organs. This 3D dilation expands the inner organs' mesh in all directions. To calculate the offset region, we compute the intersection of the main bone region with the 3D dilated inner organs. In a 3D printer with dual extruders, the offset region is printed using conductive material, while the main bone (after subtracting the offset region) and the inner organs are printed using non-conductive white PLA. Figure 4 illustrates the process of preparing this offsetting approach.

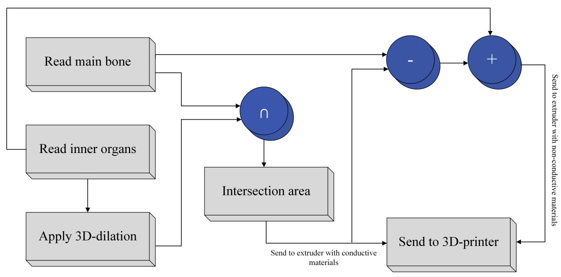

Figure 4: Process of creating the offset region and 3D print model with offset.

The offset region is analogous to the skeletonization concept in head and neck surgery. Skeletonization, in surgical techniques, refers to the method in which the surgeon carefully removes the bony structure covering vital organs such as the facial nerve, inner ear, etc. The objective is to expose these organs while maintaining their integrity, allowing the surgeon to perform the operation without risking damage to these delicate areas. The protective layer provided by the offset region improves the feedback system by notifying the user before the inner organs are injured or cut. Specifically, when the drill reaches the conductive area, the user will be alerted, indicating proximity to the inner organs. This warning allows the user to decide whether to continue drilling with a larger burr or switch to a smaller burr. Moreover, the user can choose to identify a specific organ or leave it skeletonized by cleaning the bony parts and retaining only the conductive layer. Figure 8.a shows the combination of inner organs with a protective layer, integrated into the main bone, forming the ready-to-print model. Figure 8.b depicts the 3D-printed version of this model. Figure 8.c displays the designed inner organs, while Figure 8.d adds the protective layer. Lastly, Figure 8.e separates the inner organs, protective layer, and main bone for individual visualization. Both the main bone and inner organs were printed using non-conductive material, while the protective layer was printed using conductive material. The same circuit used for intactness detection in the first design was utilized here, producing buzzer sounds and activating blinking LEDs when the drill tip touches the conductive layer.

5 RESULTS AND EXPERIMENTS

In this section, we describe the process of creating the physicalization of the temporal bone and evaluate the accuracy of the 3D-printed model by comparing its size to the .stl file (ground truth). We focus on both the segmentation of critical anatomical structures and the precision of the final 3D-printed temporal bone.

5.1 Physicalization of Temporal Bone

For 3D printing purposes, the segmentation of critical anatomical structures within the temporal bone is essential. These structures include the sigmoid sinus, facial nerve, stapes, malleus, incus, semicircular canals, cochlea, etc. Segmentation enables the accurate visualization and physicalization of these structures, which is necessary for precise 3D printing.

Two main steps are required for the physicalization process: first, segmenting the inner structures of the temporal bone using an appropriate method, and second, developing a 3D printing technique that can accurately recreate the bone's complex anatomy. The segmentation of the inner organs has already been completed, leaving only the segmentation of the bone itself. To accomplish this, we apply Hounsfield Unit (HU) thresholding, using a range of 600 to 2390 HU to isolate the bone structure from the surrounding tissues. The segmented parts then converted to 3D mesh using Marching Cubes.

Figure 5 presents the complete flowchart outlining the physicalization steps, from segmentation to mesh generation and 3D printing. The mesh created through segmentation is exported in a 3D-printable format, such as .stl. After adjusting the printer settings, the model is ready to be printed. This physical 3D model will be integrated into the feedback system described in Section 4. The feedback system, which includes a Raspberry Pi and sensors, is attached to the printed temporal bone. This system is designed to provide real-time feedback during active interaction scenarios such as surgery simulations, with the sensors detecting interactions with the bone structure during the procedure. The final setup, illustrated in Figure 6, shows the final active physicalization including 3D-printed temporal bone model, the Raspberry Pi and sensor attachments.

The 3D printing process, utilizing our MakerGear M3-ID Dual Extruder printer, takes approximately 5 hours to complete a single temporal bone model. After printing, the Raspberry Pi and sensors are connected to the model using predefined attachment points to ensure the proper integration of the feedback system into the printed structure. Additionally, a video has been provided to demonstrate the functionality of the our active Physicalization in action (see the supplementary material). This video showcases the interactive features of the system, such as the blinking LEDs and buzzer sounds, which respond to sensor input during the simulation. Furthermore, as an examplary action for applications such as surgery simulation, audio tracks guide the users through the steps of mastoidectomy surgery.

The feedback system in our active physicalization offers real-time feedback through sensory signals. One of the key advantages of this system is its ability to provide both visual and auditory cues, which can significantly assist training process.

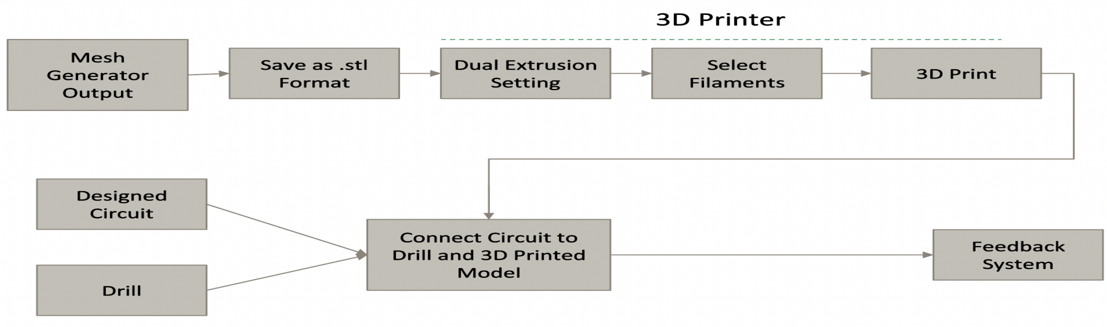

Figure 5: The steps for creating active Physicalization of the temporal bone.

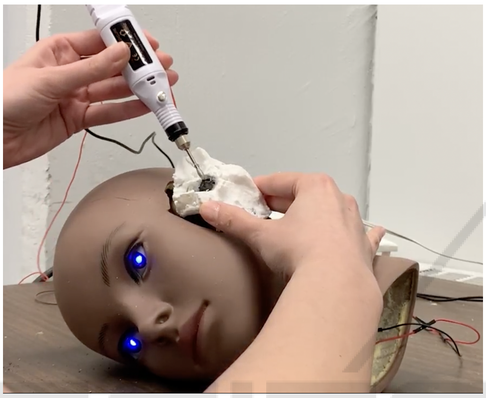

Figure 6: Feedback system Implemented in the real world.

5.2 Evaluating the Accuracy of 3D Printed Model

To assess the precision of the 3D-printed model, we first analyze cross-sections of sample bones, as shown in Figure 7. Two sample bones were printed in halves, and their dimensions were measured using a caliper. These measurements were then compared with the original dimensions of the .STL file, which were measured using the MeshLab software. The differences between these measurements, recorded in millimeters.

The measurements include assessments of the bone and the visible inner organs in the cross-section from various directions and angles, such as left to right and top to bottom. The goal is to demonstrate the accuracy of the printed models and provide an average difference to highlight the precision of the printing process. These two samples were specifically chosen because they represent the sigmoid sinus in two different parts, which enhances the reliability of the measurements. Another reason for selecting these samples is that the sigmoid sinus is a larger structure, making it easier to showcase through images. Examples of such measurements are displayed in Table 1 comparing ground truth .stl file and the 3D-printed model.

Table 1: Comparison between ground truth measurements and 3D printed images for different parts.

	Image Part	Image Part	Image Part
	SS Part-1	**SS Part-2**	**Main Bone**
ground truth	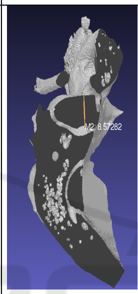	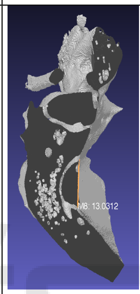	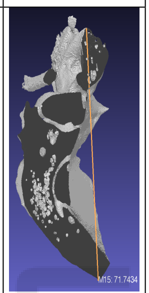
3D Printed	8.7 mm	13.4 mm	71.5 mm

As illustrated in Table 2, there are four key columns. The first column indicates the name of the anatomical landmark. The second column reports the measurements obtained from the .STL file, which serves as the ground truth. The third column provides the measurements taken from the 3D-printed cross-section. Finally, the fourth column presents the relative difference between the measurements in the second and third columns. The accuracy evaluation revealed that the 3D-printed models closely match the dimensions of the original .STL files, with a relative difference ranging from 0% to approximately 4% for most structures and an overal average of 1.48%. The larger anatomical structures, such as the sigmoid sinus, exhibited a higher degree of accuracy with minimal differences, as they were easier to replicate and measure.

Smaller structures, on the other hand, showed slightly larger deviations, particularly when the dimensions were more intricate and complex to replicate. The relative differences for these smaller features ranged between 2% and 4%.

Overall, the accuracy results confirm that the 3D-printed temporal bone models are reliable representations of the anatomical structures they replicate.

Table 2: Measurement results for two samples of printed temporal bones.

Measurement	Ground Truth	3D Printed	Rel. Diff. (%)
SS-1 (L→R)	16.83	16.9	0.42%
SS-1 (T→B)	8.57	8.7	1.52%
SS-2 (T→B)	13.03	13.4	2.83%
SS-2 (L→R)	5.20	5.3	1.92%
Main bone (Diag.)	56.81	55.9	1.60%
Main bone (T→B)	71.74	71.5	0.33%
Main bone (Peak)	6.71	7.0	4.32%
Main bone (L→R)	22.94	22.43	2.22%
Second Sample			
SS-1 (L→R)	16.3	16.2	0.61%
SS-1 (T→B)	8.64	9.0	4.17%
SS-2 (T→B)	16.51	16.3	1.27%
SS-2 (L→R)	5.83	5.9	1.20%
Main bone (L→R)	20.53	20.4	0.63%
Main bone (T→B)	72.09	72.2	0.15%
Main bone (Diag.)	57.27	57.2	0.12%
Main bone (Peak)	7.27	7.3	0.41%
Overall Avg.			**1.48%**

However, there is room for further improvement, particularly in refining the mesh smoothing process and optimizing the segmentation of smaller anatomical features. These enhancements would help reduce the occurrence of minor artifacts and further improve the fidelity of the printed models.

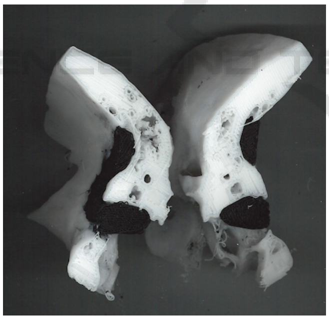

Figure 7: Partially 3D printed bones used for verifying measurements.

6 CONCLUSIONS

In this paper, we have developed an active physicalization model with interactive features enabled by conductive materials and a controller. The model employs conductive 3D filaments to create sensors that trigger a feedback system upon activation. This interactive model is applicable to a range of physicalized models where the internal structure is critical.

As a case study, we considered utelizing the Physicalization for feedback in drilling or cutting actions. When a modified surgical drill comes into contact with these conductive-material-printed inner organs, the feedback system is triggered, producing responses such as a buzzer sound or blinking LEDs.

The 3D model was fabricated using an FDM 3D printer, with white PETG for the main bone structure and conductive PLA for the inner organs. In an alternative design, both the main bone structure and inner organs were printed using white PETG, with a protective layer of conductive PLA added. In both designs, the conductive areas acted as sensors to detect the proximity of surgical tools to inner organs. The feedback system, powered by a Raspberry Pi, was further enhanced with oral instructions to provide supplementary guidance during surgical rehearsals.

By integrating conductivity, electronics, controllers, and 3D printing technologies, we have developed an interactive model capable of providing real-time feedback. The case study presented demonstrates the adaptability and versatility of our approach, which can be extended to various disciplines beyond temporal bone surgery.

In future work, researchers can explore the application of active physicalization in clinical settings, particularly for surgical simulation and training. This interactive physicalization model holds potential for any application requiring real-time feedback, such as enhancing precision in delicate procedures or industrial tasks. Further development could focus on improving the accuracy of 3D-printed models and implementing more systematic methods to compare them against ground truth data. This would provide a robust framework for validating the efficacy of physicalized models across various disciplines.

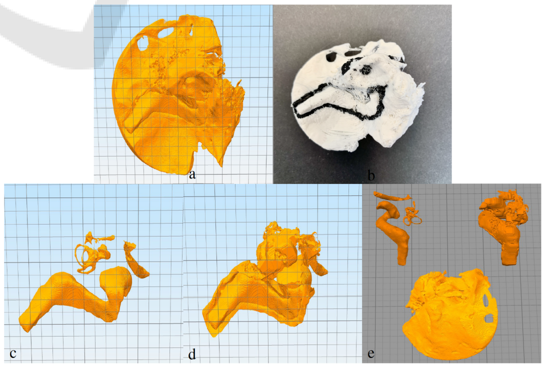

Figure 8: A) Combined model of inner organs, protective layer, and main bone. b) 3D-printed model. c) Inner organs. d) Inner organs with protective layer. e) Separate components: inner organs, protective layer, and main bone.

ACKNOWLEDGEMENTS

We would like to thank Dr. Joseph Dort and Dr. Sonny Chan for providing the temporal bone dataset essential to this research. We also appreciate Farima Golchin's assistance with figure styling and Katayoun Etemad's guidance in creating physical models. This work was supported by the Natural Sciences and Engineering Research Council of Canada (NSERC).

REFERENCES

Allahverdi, K., Djavaherpour, H., Mahdavi-Amiri, A., and Samavati, F. (2018). Landscaper: A modeling system for 3d printing scale models of landscapes. In *Computer Graphics Forum*, volume 37, pages 439–451. Wiley Online Library.

Ang, A. J. Y., Chee, S. P., Tang, J. Z. E., Chan, C. Y., Tan, V. Y. J., Lee, J. A., Schrepfer, T., Ahamed, N. M. N., and Tan, M. B. (2024). Developing a production workflow for 3d-printed temporal bone surgical simulators. *3D Printing in Medicine*, 10(1):1–15.

Ang, K. D., Samavati, F. F., Sabokrohiyeh, S., Garcia, J., and Elbaz, M. S. (2019). Physicalizing cardiac blood flow data via 3d printing. *Computers & Graphics*, 85:42–54.

Bao, G., Yang, P., Yi, J., Peng, S., Liang, J., Li, Y., Guo, D., Li, H., Ma, K., and Yang, Z. (2023). Full-sized realistic 3d printed models of liver and tumour anatomy: A useful tool for the clinical medicine education of beginning trainees. *BMC Medical Education*, 23(1):574.

Barber, S. R., Wong, K., Kanumuri, V., Kiringoda, R., Kempfle, J., Remenschneider, A. K., Kozin, E. D., and Lee, D. J. (2018). Augmented reality, surgical navigation, and 3d printing for transcanal endoscopic approach to the petrous apex. *OTO open*, 2(4):2473974X18804492.

Barbosa, C., Sousa, T., Monteiro, W., Araújo, T., and Meiguins, B. (2023). Enhancing color scales for active data physicalizations. *Applied Sciences*, 14(1):166.

Boem, A. and Iwata, H. (2018). "it's like holding a human heart": the design of vital+ morph, a shape-changing interface for remote monitoring. *AI & SOCIETY*, 33(4):599–619.

Chung, Y.-J., Park, J.-M., Kim, T.-H., Ahn, J.-S., Cha, H.-S., and Lee, J.-H. (2018). 3d printing of resin material for denture artificial teeth: Chipping and indirect tensile fracture resistance. *Materials*, 11(10):1798.

Cohen, J. and Reyes, S. A. (2015). Creation of a 3d printed temporal bone model from clinical ct data. *American Journal of Otolaryngology*, 36(5):619–624.

Djavaherpour, H., Samavati, F., Mahdavi-Amiri, A., Yazdanbakhsh, F., Huron, S., Levy, R., Jansen, Y., and Oehlberg, L. (2021). Data to physicalization: A survey of the physical rendering process. In *Computer Graphics Forum*, volume 40, pages 569–598. Wiley Online Library.

Domysche, M., Terekhov, S., Astapenko, O., Vefelev, S., and Tatarina, O. (2024). The use of 3d printers in dental production practice: Possibilities for the manufacture of individual dental prostheses and elements.

Etemad, K., Samavati, F., and Dawson, P. (2023). Multiscale physicalization of polar heritage at risk in the western canadian arctic. *The Visual Computer*, 39(5):1717–1729.

Fedorov, A., Beichel, R., Kalpathy-Cramer, J., Finet, J., Fillion-Robin, J.-C., Pujol, S., Bauer, C., Jennings, D., Fennessy, F., Sonka, M., et al. (2012). 3d slicer as an image computing platform for the quantitative imaging network. *Magnetic resonance imaging*, 30(9):1323–1341.

Flowers, P. F., Reyes, C., Ye, S., Kim, M. J., and Wiley, B. J. (2017). 3d printing electronic components and circuits with conductive thermoplastic filament. *Additive Manufacturing*, 18:156–163.

Freiser, M. E., Ghodadra, A., Hirsch, B. E., and McCall, A. A. (2019). Evaluation of 3d printed temporal bone models in preparation for middle cranial fossa surgery. *Otology & Neurotology*, 40(2):246–253.

Guo, X.-Y., He, Z.-Q., Duan, H., Lin, F.-H., Zhang, G.-H., Zhang, X.-H., Chen, Z.-H., Sai, K., Jiang, X.-B., Wang, Z.-N., et al. (2020). The utility of 3-dimensional-printed models for skull base meningioma surgery. *Annals of Translational Medicine*, 8(6).

Haas, J. K. (2014). A history of the unity game engine. *Worcester Polytechnic Institute*.

Haffner, M., Quinn, A., Hsieh, T.-y., Strong, E. B., and Steele, T. (2018). Optimization of 3d print material for the recreation of patient-specific temporal bone models. *Annals of Otology, Rhinology & Laryngology*, 127(5):338–343.

Hochman, J. B., Kraut, J., Kazmerik, K., and Unger, B. J. (2014). Generation of a 3d printed temporal bone model with internal fidelity and validation of the mechanical construct. *Otolaryngology–Head and Neck Surgery*, 150(3):448–454.

Hou, R., Hui, X., Xu, G., Li, Y., Yang, X., Xu, J., Liu, Y., Zhu, M., Zhu, Q., and Sun, Y. (2024). Use of 3d printing models for donor tooth extraction in autotransplantation cases. *BMC Oral Health*, 24(1):179.

Houben, S., Golsteijn, C., Gallacher, S., Johnson, R., Bakker, S., Marquardt, N., Capra, L., and Rogers, Y. (2016). Physikit: Data engagement through physical ambient visualizations in the home. In *Proceedings of the 2016 CHI conference on human factors in computing systems*, pages 1608–1619.

Huang, X., Liu, Z., Wang, X., Li, X.-d., Cheng, K., Zhou, Y., and Jiang, X.-b. (2019). A small 3d-printing model of macroadenomas for endoscopic endonasal surgery. *Pituitary*, 22:46–53.

Huron, S., Gourlet, P., Hinrichs, U., Hogan, T., and Jansen, Y. (2017). Let's get physical: Promoting data physicalization in workshop formats. In *Proceedings of the 2017 Conference on Designing Interactive Systems*, pages 1409–1422.

Iannella, G., Pace, A., Mucchino, A., Greco, A., De Virgilio, A., Lechien, J. R., Maniaci, A., Cocuzza, S., Perrone, T., Messineo, D., et al. (2024). A new 3d-printed temporal bone:'the sapiens'—specific anatomical printed-3d-model in education and new surgical simulations. *European Archives of Oto-Rhino-Laryngology*, pages 1–10.

Jackler, D. and Gralapp, C. (2024). Oto surgery atlas – department of ohns. https://otosurgeryatlas.stanford.edu/. Last accessed October 2024, Images belong to the illustrators and the Stanford Otolaryngology — Head & Neck Surgery Department, permission obtained from illustrator (Christine Gralapp).

Jansen, Y., Dragicevic, P., Isenberg, P., Alexander, J., Karnik, A., Kildal, J., Subramanian, S., and Hornbæk, K. (2015). Opportunities and challenges for data physicalization. In *Proceedings of the 33rd Annual ACM Conference on Human Factors in Computing Systems*, pages 3227–3236.

Jeising, S., Liu, S., Blaszczyk, T., Rapp, M., Beez, T., Cornelius, J. F., Schwerter, M., and Sabel, M. (2024). Combined use of 3d printing and mixed reality technology for neurosurgical training: getting ready for brain surgery. *Neurosurgical Focus*, 56(1):E12.

Karolus, J., Brass, E., Kosch, T., Schmidt, A., and Wozniak, P. (2021). Mirror, mirror on the wall: Exploring ubiquitous artifacts for health tracking. In *Proceedings of the 20th International Conference on Mobile and Ubiquitous Multimedia*, pages 148–157.

Kwok, S. W., Goh, K. H. H., Tan, Z. D., Tan, S. T. M., Tjiu, W. W., Soh, J. Y., Ng, Z. J. G., Chan, Y. Z., Hui, H. K., and Goh, K. E. J. (2017). Electrically conductive filament for 3d-printed circuits and sensors. *Applied Materials Today*, 9:167–175.

Lane, J. I. and Witte, R. J. (2009). The temporal bone. *An imaging atlas. Heidelberg: Springer*.

Longfield, E. A., Brickman, T. M., and Jeyakumar, A. (2015). 3d printed pediatric temporal bone: a novel training model. *Otology & Neurotology*, 36(5):793–795.

LOZANO-HEMMER (2011). Tape recorders: Time-measuring tapes. http://dataphys.org/list/tape-recorders-measure-time-instead-of-distance/.

McJunkin, J. L., Jiramongkolchai, P., Chung, W., Southworth, M., Durakovic, N., Buchman, C. A., and Silva, J. R. (2018). Development of a mixed reality platform for lateral skull base anatomy. *Otology & neurotology: official publication of the American Otological Society, American Neurotology Society [and] European Academy of Otology and Neurotology*, 39(10):e1137.

Mossman, C., Samavati, F. F., Etemad, K., and Dawson, P. (2023). Mobile augmented reality for adding detailed multimedia content to historical physicalizations. *IEEE Computer Graphics and Applications*, 43(3):71–83.

Pahr, D., Ehlers, H., Wu, H.-Y., Waldner, M., and Raidou, R. G. (2024). Investigating the effect of operation mode and manifestation on physicalizations of dynamic processes. *arXiv preprint arXiv:2405.09372*.

Park, J. H., Lee, Y.-B., Kim, S. Y., Kim, H. J., Jung, Y.-S., and Jung, H.-D. (2019). Accuracy of modified cad/cam generated wafer for orthognathic surgery. *PloS one*, 14(5):e0216945.

Reich, S., Berndt, S., Kühne, C., and Herstell, H. (2022). Accuracy of 3d-printed occlusal devices of different volumes using a digital light processing printer. *Applied Sciences*, 12(3):1576.

Roo, J. S., Gervais, R., Lainé, T., Cinquin, P.-A., Hachet, M., and Frey, J. (2020). Physio-stacks: Supporting communication with ourselves and others via tangible, modular physiological devices. In *22nd International Conference on Human-Computer Interaction with Mobile Devices and Services*, pages 1–12.

Rose, A. S., Webster, C. E., Harrysson, O. L., Formeister, E. J., Rawal, R. B., and Iseli, C. E. (2015). Preoperative simulation of pediatric mastoid surgery with 3d-printed temporal bone models. *International journal of pediatric otorhinolaryngology*, 79(5):740–744.

Sauvé, K., Bakker, S., and Houben, S. (2020). Econundrum: Visualizing the climate impact of dietary choice through a shared data sculpture. In *Proceedings of the 2020 ACM Designing Interactive Systems Conference*, pages 1287–1300.

Schroeder, W. J., Lorensen, B., and Martin, K. (2004). *The visualization toolkit: an object-oriented approach to 3D graphics*. Kitware.

ScienceDirect (2024). Hounsfield scale - an overview. https://www.sciencedirect.com/topics/medicine-and-dentistry/hounsfield-scale. Accessed: October 21, 2024.

Sun, Z., Wong, Y. H., and Yeong, C. H. (2023). Patient-specific 3d-printed low-cost models in medical education and clinical practice. *Micromachines*, 14(2):464.

Suzuki, R., Taniguchi, N., Uchida, F., Ishizawa, A., Kanatsu, Y., Zhou, M., Funakoshi, K., Akashi, H., and Abe, H. (2018). Transparent model of temporal bone and vestibulocochlear organ made by 3d printing. *Anatomical science international*, 93(1):154–159.

Takahashi, K., Morita, Y., Ohshima, S., Izumi, S., Kubota, Y., Yamamoto, Y., Takahashi, S., and Horii, A. (2017). Creating an optimal 3d printed model for temporal bone dissection training. *Annals of Otology, Rhinology & Laryngology*, 126(7):530–536.

Tan, L., Wang, Z., Jiang, H., Han, B., Tang, J., Kang, C., Zhang, N., and Xu, Y. (2022). Full color 3d printing of anatomical models. *Clinical Anatomy*, 35(5):598–608.

Wan, D., Wiet, G. J., Welling, D. B., Kerwin, T., and Stredney, D. (2010). Creating a cross-institutional grading scale for temporal bone dissection. *The Laryngoscope*, 120(7):1422–1427.

Wanibuchi, M., Noshiro, S., Sugino, T., Akiyama, Y., Mikami, T., Iihoshi, S., Miyata, K., Komatsu, K., and Mikuni, N. (2016). Training for skull base surgery with a colored temporal bone model created by three-dimensional printing technology. *World neurosurgery*, 91:66–72.

Yushkevich, P. A., Piven, J., Hazlett, H. C., Smith, R. G., Ho, S., Gee, J. C., and Gerig, G. (2006). User-guided 3d active contour segmentation of anatomical structures: significantly improved efficiency and reliability. *Neuroimage*, 31(3):1116–1128.